

## Optimal Decentralized SOP Allocation in the MAADN with Autonomous Self-Interested Agents

Hiba Zuhair<sup>1</sup>, Hamdi Abdi<sup>1,\*</sup>, Hassan Moradi<sup>1</sup>

<sup>1</sup> Department of Electrical Engineering, Razi University, Kermanshah 67144-14971, Iran

### ARTICLE INFO

### ABSTRACT

#### Article history:

Received 18 July 2023

Received in revised form 05 August 2023

Accepted 06 September 2023

#### Keywords:

Multi-area active distribution network

Autonomy

Decentralized planning

SOP

Renewable distributed generators.



**Copyright:** © 2023 by the authors. Submitted for possible open access publication under the terms and conditions of the Creative Commons Attribution (CC BY) license (<https://creativecommons.org/licenses/by/4.0/>)


The non-dispatchable and intermittent nature of renewable distributed generators, i.e., photovoltaic and wind power plants, can lead to voltage variations and disruption in energy exchanges, especially in multi-area active distribution networks. Therefore, to manage inter-area energy exchanges in the presence of high penetration level of renewable distributed generators, the flexibility and controllability of the grid should be increased by using soft open points. However, the investment cost of soft open points is very high. On the other hand, soft open points affect the energy transactions in the multi-area active distribution network, so, they should be optimally allocated with the satisfaction of all the network areas. In this research, for the first time, a new decentralized framework for optimal siting and sizing of soft open points is developed, considering the self-interested nature of the areas and preserves their autonomy and information privacy. By using the suggested framework, different areas can negotiate with each other on the location and size of soft open points, and the relatively equal share of their investment costs. The correctness of the proposed decentralized planning model is confirmed by two case studies in MATLAB. The results confirm that the proposed method can allocate the share of each area based on the profit from new SOPs and also preserve the privacy, in both case studies.

### Abbreviations

		NOP	Normally opened point
		CDGs	Controllable distributed generator
RDG	Renewable distributed generator	LSM	Local scheduling model
WT	Wind turbine	FI	Fitness index
PV	Photovoltaic	NFI	Net fitness index
ADN	Active distribution network	GA	Genetic algorithm
DN	Distribution network	PSO	Particle swarm optimization
DER	Distributed energy resource	UN	Upstream network
SOP	Soft open point	Sets and Indices:	
MISOCP	Mixed integer second-order cone programming	$m/a$	The index of area

<sup>1</sup> \* Corresponding author

E-mail address: [hamdiabdi@gmail.com](mailto:hamdiabdi@gmail.com)

 <https://orcid.org/0000-0002-7625-0036>

<http://dx.doi.org/10.48308/ijrtei.2023.235416.1043>

$A_m$	Area $m$	$I_{t,ij}^m$	The square current amplitude of the line $ij$
$X^m$	The set of variables	$Pls_{t,s}^m$	The active power loss of SOP $s$
$g^m(X^m)/f^m(X^m)$	The equality/inequality constraints in the LSM of $A_m$	$Psm_{1/2,t,s}^m$	The auxiliary variable describing the absolute value of $PS_{1/2,t,s}^m$
$G^m$	The set of all CDGs in $A_m$	$SS_{max,s}^m$	The maximum apparent power of SOPs
$T$	The set of all-time intervals in a year	$Pc_{t,g}^m/Qc_{t,g}^m/Sc_{t,g}^m$	The generated active/reactive/apparent power of CDG $g$
$t/g/m$	Index of time/CDG/area	$Pb_{t,ij}^m/Qb_{t,ij}^m/Sb_{t,ij}^m$	The injected active/reactive/apparent power to line $ij$
$M$	The set of MAADN areas	$v_{t,j}^m$	The voltage magnitude of the node $j$
$B^m$	Distribution lines set	$\eta_p^m$	The FI of the area $m$ at the plan $p$
$S^m/s$	Set/index of the SOP	$C_{to,p}^m$	The annual operating cost of the area $m$ at plan $p$
$S_{1/2,j}^m$	Set of SOPs connected to node $j$ among the converter 1/2	$C_p^{SOP}$	The annual investment cost of new SOPs in the plan $p$
$Dn_j^m$	Downstream nodes set of node $j$	$F_p$	The NFI of the plan $p$
$N^m$	The set of all nodes in $A_m$	$SS_{max,s}^p$	The nominal apparent power of SOP $s$ in plan $p$
$p$	The index of the plan	$C_{SOP}^m$	The annual SOP's investment cost of the area $m$
$S_p$	The set of all allocated SOPs in the plan $p$		
$M_p$	The set of areas with positive FI in the plan $p$		
Variables:			
$C_{to}^m$	The total annual net cost	Parameters:	
$C_{CDG}^m$	The operation cost of controllable DGs	$a_g^m, b_g^m$ and $c_g^m$	The cost coefficients of CDG
$C_{UN}^m$	The total annual cost of importing electrical power from the UN	$\tau$	The duration of each time interval
$C_A^m$	Importing power cost from other areas	$\lambda p_t/\lambda q_t$	The unit price of active and reactive power
$C_l^m$	The total energy loss cost is on the planning horizon.	$\lambda_t^{ADN}$	The price of inter-area energy transactions in the MAADN
$Pun_{t,sl}^m/Qun_{t,sl}^m$	The active/reactive imported power from the UN	$r_{ij}/x_{ij}$	The resistance/reactance of the line $ij$
$Pc_{t,g}^m/Qc_{t,g}^m$	The generated active and reactive power of the controllable DG	$Z_{1/2,s}^m$	The loss coefficient of converter 1/2 of SOP $s$
$p_t^{a2m}$	The exported active power from area $a$ to area $m$	$Pc_{min,g}^m/Pc_{max,g}^m$	The active power generation limitations of CDG $g$
$C_{IB}^m/C_{IS}^m$	The energy losses cost of distribution lines/SOPs	$Sc_{max,g}^m$	The maximum apparent power generated by the $g$ th CDG
$PF_{min,g}^m$	The minimum power factor of the generated power of CDG $g$	$C_{to}^{m*}$	The annual operating cost of the area $m$ without new SOPs
$Pp_{t,j}^m/Pw_{t,j}^m$	The generated power of PV/WT in node $j$	$c^{SOP}$	The per unit investment cost of the SOP
$Pl_{t,j}^m/Qt_{t,j}^m$	The load demand of the node $j$	$lf$	The lifetime of the SOP
$v_{min}/v_{max}$	The minimum/maximum allowed square voltage magnitude of nodes	$dr$	The discount rate

### 1. Introduction

To achieve the goals of reducing environmental emissions, renewable distributed generators (RDGs), i.e., wind turbines (WTs) and photovoltaics (PVs), have received extensive attention [1]. By moving towards low-

carbon energy systems, it is expected that RDG's penetration in the power grids will increase significantly [2].

In this regard, the distribution network (DN) operation becomes more complex by increasing the penetration

level of distributed energy resources (DERs) [3]. Also, a significant increase in RDGs brings serious problems for active DNs (ADNs) because of their intermittent nature and lack of flexibility [4]. In such situations, the flexibility and controllability of the ADN should be increased using the soft open point (SOP) to increase the hosting capacity for RDGs. The SOP consists of two AC/DC converters connected back-to-back through a DC link. SOPs control the reactive and active power flow and compensate for the reactive power continuously [5].

The effectiveness of SOPs in improving ADN performance has been shown in many studies, such as [6] and [7]. In [8], the power losses and voltage deviation of the ADN were deducted using SOPs. The ability of SOP to reduce phase imbalance is investigated in [9]. In [10], the capability of SOP on the DN predictability is examined. In [11], the SOP has been utilized to improve energy accommodation interaction between the ADN and multiple electricity-driven central energy stations. In [12], a real-time voltage control method for SOPs is addressed to reduce voltage variations and power losses in highway transportation power supply grids. To enhance distribution network flexibility, an edge intelligence-based strategy to online schedule of SOPs is described in [13]. In [4], an expansion planning model is proposed for SOP-based DNs considering the charging behavior of electric vehicles. This model can reduce planning and electric vehicle navigation costs, simultaneously. However, this model is a single-agent centralized model that is not suitable for the MAADN.

The effect of inter-area SOPs in improving energy transactions of DERs between autonomous areas in the MAADN has been investigated in [14]. However, the self-interested nature and self-own economy of areas are neglected. In [15], the island operation scheduling of the ADN is optimized in the presence of SOPs to improve the ADN resiliency after extreme faults. In [16] and [17], two resilience-oriented operational and planning models are proposed to schedule and allocate SOPs optimally. Because of the high investment cost of SOPs [18], their sizing and siting should be optimally determined considering both technical and economic aspects. In this regard, several frameworks have been proposed. In [19], a centralized mixed-integer non-linear planning approach is suggested to optimal allocation of SOPs. In this model, the objective function is to minimize the DN's annual expense, which includes annual operational cost, energy loss cost, and investment cost of the SOP. A bi-level, coordinated, centralized planning model for simultaneous siting and sizing of converter-based SOPs and Distributed Generators is presented in [20]. The total cost of the DN and the voltage unbalance and power loss have been minimized in the lower and upper levels, respectively. To solve this bi-level model, the authors have transformed it into a mixed integer second-order cone programming (MISOCP) problem. In [21], a stochastic planning method is suggested to allocate the SOP in the ADN, considering the network reconfiguration.

To improve the post-fault restoration ability of the DN and reduce its power loss, a practical SOP-planning method is addressed in [18]. In this model, due to the high investment cost, it is assumed that only one SOP can be

installed in the DN and only at its Normally Opened Points (NOPs). To maximize the restored loads following a severe fault, an SOP-based service restoration strategy in two-stage is addressed in [22], which maximizes the recovered load by coordinating the existing DGs and SOPs. However, it is not suitable to specify the optimal size and site of new SOPs.

Authors in [23] have proposed a cost-benefit analysis methodology to analyse five value streams of an SOP, including enabling flexibility services, reliability increasing, reducing curtailment of RDGs, power loss reduction, and reinforcement deferral. To enhance the DN resilience against typhoons, a coordinated planning-operation strategy for SOP, battery storage systems, and DGs is proposed in [24]. A stochastic multi-objective model for SOP planning, includes RDGs power fluctuations and load growth uncertainties, is proposed in [25].

The review of the literature indicates that the current SOP allocation methods are only suitable for single-agent networks such as the DN or ADN, which operate by unique operators, i.e., the DSO. In these methods, the size and site of SOPs are optimized centrally from the viewpoint of the DSO, considering only its goals, such as energy loss reduction and resiliency enhancement. However, the MAADN is a multi-agent network in which each of its areas is an autonomous agent operated independently by its private policy. Therefore, the centralized SOP siting and sizing methods cannot be applied in the MAADN.

Table 1 summarizes some of the SOP allocation frameworks in order to draw attention to the novelties of this paper. It is evident that the proposed strategy is the

only planning framework that satisfies all the SOP allocation requirements in the MAADN. The main contributions of the proposed SOP-allocation approach are listed in the following:

- For the first time, a fully decentralized planning method is addressed for optimal siting and sizing of SOPs in the MAADN.
- The agents in the MAADN are modeled as self-interested entities, considering their independence, operational autonomy, and privacy.
- The site and size of SOPs are determined by contributing all the agents.
- The SOP investment cost is divided fairly between the MAADN areas according to their declared profits from installing the new SOPs.
- All problem constraints, include voltage amplitude boundaries, the thermal threshold of distribution lines, controllable distributed generators (CDGs) constraints, and SOPs operational limitations are modelled without the need for a central coordinator.”

In the reminder of this paper, the problem formulation is represented in Section 2. The proposed approach for SOP planning is represented in Section 3. Then, the effectiveness of this method is evaluated with various simulation studies in Section 4. Finally, the conclusion is represented in Section 5.

Table 1. Comparison of SOP planning methods.

Ref	Type of planning	Model	Agent privacy	Agent independence	SOP loss	Power transaction	Investment cost sharing
[4]	Centralized (one agent)	MISOCP	×	×	✓	×	×
[19]	Centralized (one agent)	MISOCP	×	×	✓	×	×
[20]	Centralized (one agent) bi-level optimization		×	×	✓	×	×
[18]	Centralized (one agent)	MISOCP	×	×	×	×	×
[23]	Centralized (one agent)	second-order cone programming	×	×	✓	×	×
[24]	Centralized (one agent)	two-stage robust optimization	×	×	×	×	×
[25]	Centralized (one agent)	mixed-integer linear programming	×	×	✓	×	×
This work	Decentralized (multi-agent)	MISOCP	✓	✓	✓	✓	✓

## 2. The problem formulation

In this section, the proposed SOP allocation model is represented mathematically.

### 2.1. Assumptions and goals

This paper assumes that the location and nominal capacity of new RDGs in each area of the MAADN are predefined parameters. In other words, based on geographical conditions and available budget, each agent has planned independently the development scheme of RDGs in its area. For example, a MAADN with four autonomous agents  $A_1$  to  $A_4$  is shown in Fig. 1.

It depicts that the operator of each area investigates the best SOP allocation plan. Since the SOP installation affects the power scheduling in all areas, the final plan must be specified determined by the agreement of all areas. The proposed method aims to site and size new SOPs in this MAADN to maximize its net profit in the presence of a high penetration level of RDGs. However, as shown in this figure, each area is planned independently by its private agent.

These agents are in contact with each other, but they do not share their private information, such as local DER data. So, centralized SOP allocation methods are not applicable. Therefore, a decentralized planning framework is required to determine the optimal SOP

allocation. In this method, each share of each area in paying the SOP investment costs should be determined with the consent of that area. In such a way that all the investment costs are covered.

### 2.2. Local scheduling model

In the MAADN, each area wants to minimize its costs according to its unique Local Scheduling Model (LSM). In this paper, to independently model the annual operational cost of each area, a general LSM is formulated from the viewpoint of area  $m$  ( $A_m$ ) in (1). Note that, for privacy reasons, the LSM of area  $m$  ( $A_m$ ) is visible only for itself. The superscript  $m$  is used in this LSM To emphasize privacy,

$$\begin{aligned} \min_{X^m} C_{to}^m \\ \text{subject to } \begin{cases} g^m(X^m) \leq 0 \\ f^m(X^m) = 0 \end{cases} \end{aligned} \quad (1)$$

Where,  $X^m$  is the set of variables,  $f^m(X^m)$  and  $g^m(X^m)$  are inequality and equality constraints in the LSM of  $A_m$ .  $C_{to}^m$  is the total annual net cost  $A_m$ , which is defined in (2).

$$C_{to}^m = C_{CDG}^m + C_{UN}^m + C_A^m + C_l^m \quad (2)$$

$C_{CDG}^m$  is the cost of CDGs operation in the annual scheduling horizon,  $C_{UN}^m$  is the total annual cost of importing net electrical power from the UN,  $C_A^m$  is the importing power cost from other areas, and  $C_l^m$  is the total energy loss cost in the planning horizon. The details of the operation costs are addressed in the following sections.

#### 2.2.1 The controllable distributed generator cost

In (3),  $C_{CDG}^m$  is defined as a quadratic function as follows:

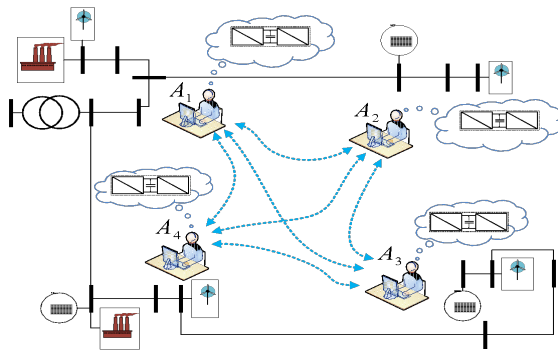


Fig. 1. SOP-allocation in the MAADN with self-interested agents.

$$C_{CDG}^m = \tau \sum_{t \in T} \sum_{g \in G^m} (a_g^m \times P_{c,t,g}^{m2} + b_g^m \times P_{c,t,g}^m + c_g^m) \quad (3)$$

$a_g^m$ ,  $b_g^m$  and  $c_g^m$  are the cost coefficients, and  $P_{c,t,g}^m$  and  $Q_{c,t,g}^m$  are the active and reactive generated power of CDG  $g$  in time intervals  $t$ , respectively.  $G^m$  is a set containing all the CDGs in  $A_m$ ,  $T$  represents the scheduling horizon, which is a set containing all time intervals in a year, and  $\tau$  is the duration of each interval.

### 2.2.2 The Cost of importing power from the upstream grid

If  $A_m$  connected to the UN, the cost of importing power from the upstream network ( $C_{UN}^m$ ) should be calculated by (4); otherwise  $C_{UN}^m = 0$  [26].

$$C_{UN}^m = \tau \sum_{t \in T} (\lambda p_t \times P_{un,t,sl}^m + \lambda q_t \times Q_{un,t,sl}^m) \quad (4)$$

$P_{un,t,sl}^m$  and  $Q_{un,t,sl}^m$  are imported powers from the UN, and  $\lambda p_t$  and  $\lambda q_t$  are respectively their unit prices in time  $t$ . The UN announces these prices. Note that in this paper,  $P$ , and  $Q$  refer to active and reactive powers. Also, superscript  $m$  refers to  $A_m$ .

### 2.2.3 The cost of importing power from other areas

In the MAADN, the area  $m$  can import/export power from/to the other areas. Given that the areas are private and belong to different autonomous agents, the cost of energy exchange between them should be considered in the scheduling. The net cost of importing power from the other area to the area  $m$  is formulated in (5).

$$C_A^m = \tau \sum_{t \in T} \sum_{a \in M | a \neq m} (\lambda_t^{ADN} \times P_t^{a2m}) \quad (5)$$

Where  $a$  is the index, and  $M$  is the set of MAADN areas.  $P_t^{a2m}$  is the exported active power from area  $a$  to area  $m$  in  $t$ th time interval.  $\lambda_t^{ADN}$  is the price of inter-area energy transactions in the MAADN, which is a predefined parameter.

### 2.2.4 The cost of power losses

$C_l^m$  is formulated in (6) as the sum of two parts [14].

$$C_l^m = C_{lB}^m + C_{lS}^m \quad (6)$$

$C_{lB}^m$  and  $C_{lS}^m$  are the total cost of energy losses of distribution lines and SOPs, which are defined in (7) and (8), respectively.

$$C_{lB}^m = \tau \sum_{t \in T} \left( \lambda p_t \times \sum_{ij \in B^m} (r_{ij} \times I_{t,ij}^m) \right) \quad (7)$$

$$C_{lS}^m = \tau \sum_{t \in T} \left( \lambda p_t \times \sum_{s \in S^m} (Pls_{t,s}^m) \right) \quad (8)$$

$r_{ij}$  is the resistance and  $I_{t,ij}^m$  is the square current amplitude of line  $ij$  in time  $t$ ,  $B^m$  is the set of distribution lines, and  $Pls_{t,s}^m$  is the active power loss of SOP  $s$  in time interval  $t$ , which is defined in (9).

In the following sections, the operational constraints are presented.

### 2.2.5 Soft open point constraints

SOP operational constraints are as follows [14]:

$$P_{S1,t,s}^m + P_{S2,t,s}^m + Pls_{t,s}^m = 0 \quad \forall t \in T, \forall s \in S^m \quad (9)$$

$$Pls_{t,s}^m = Zl_{1,s}^m \times Psm_{1,t,s}^m + Zl_{2,s}^m \times Psm_{2,t,s}^m \quad \forall t \in T, \forall s \in S^m \quad (10)$$

$$P_{S1/2,t,s}^m \leq Psm_{1/2,t,s}^m \quad \forall t \in T, \forall s \in S^m \quad (31)$$

$$-P_{S1/2,t,s}^m \leq Psm_{1/2,t,s}^m \quad \forall t \in T, \forall s \in S^m \quad (42)$$

$$\|P_{S1/2,t,s}^m \quad Q_{S1/2,t,s}^m\|_2 \leq Ss_{max,s}^m \quad \forall t \in T, \forall s \in S^m \quad (53)$$

Where (9) represents the active power balance rule for the SOP. In (10),  $Pls_{t,s}^m$  is defined as the sum of power losses of converter 1 and 2. In this paper, subscripts 1 and 2 refer to converters 1 and 2, respectively. So,  $Zl_{1/2,s}^m$  the loss coefficient of converter 1/2 of SOP  $s$ .  $Psm_{1/2,t,s}^m$  is the absolute value of  $P_{S1/2,t,s}^m$ , which is defined by equations (11) and (12). The nominal power of SOP is stated in (13), which  $Ss_{max,s}^m$  is the maximum apparent power of SOPs.

### 2.2.6 Controllable distributed generator constraints

The generated power limitations of CDGs are respectively presented in (14)-(16) for the active, reactive, and apparent powers [26].

$$P_{Cmin,g}^m \leq P_{c,t,g}^m \leq P_{Cmax,g}^m \quad \forall t \in T, \forall g \in G^m \quad (64)$$

$$-P_{Ct,g}^m \times \tan(\cos^{-1}(PF_{min,g}^m)) \leq Q_{c,t,g}^m \leq P_{Ct,g}^m \times \tan(\cos^{-1}(PF_g^m)) \quad \forall t \in T, \forall g \in G^m \quad (75)$$

$$\|P_{Ct,g}^m, Q_{c,t,g}^m\|_2 \leq S_{Cmax,g}^m \quad \forall t \in T, \forall g \in G^m \quad (86)$$

Where  $P_c$ ,  $Q_c$ , and  $S_c$  refer to the generated active, reactive, and apparent powers, respectively, and  $PF$

refers to the power factor. The subscripts *max* and *min* refer to the maximum and minimum allowed values, respectively.

### 2.2.7 Exchanged power limitation

According to (17), the imported power from the UN should not exceed its maximum limit ( $S_{un,max,j}$ ) [27].

$$\|P_{un,t,j}^m, Q_{un,t,j}^m\|_2 \leq S_{un,max,j} \quad \forall t \in T, \forall j \in N^m$$

$N^m$

The injected apparent power to each line and its current is limited in (18) and (19), respectively.

$$\|P_{t,ij}^m, Q_{t,ij}^m\|_2 \leq S_{b,max,ij} \quad \forall t \in T, \forall ij \in B^m$$

$$0 \leq I_{t,ij}^m \leq I_{max,ij}^m \quad \forall t \in T, \forall ij \in B^m$$

Where  $P_b$ ,  $Q_b$ , and  $S_b$  refer to injected active, reactive, and apparent power to the distribution line.

### 2.2.8 AC load flow constraints

Equations (20) and (21) represent power balance constraints for node  $j$  in the per cent of SOPs and renewable power generation. Note that these equations are formulated from the viewpoint of  $A_m$ .

$$P_{b,t,ij}^m + \sum_{s \in S_{1/2,j}^m} P_{S_{1/2,t,s}}^m + P_{p,t,j}^m + P_{w,t,j}^m + P_{c,t,j}^m + P_{un,t,j}^m = r_{ij} \times I_{t,ij}^m + P_{l,t,j}^m \quad (20)$$

$$+ \sum_{k \in Dn_j^m} P_{b,t,jk}^m \quad \forall t \in T, \forall j \in N^m$$

$$Q_{b,t,ij}^m + \sum_{s \in S_{1/2,j}^m} Q_{S_{1/2,t,s}}^m + Q_{c,t,j}^m + Q_{un,t,j}^m = x_{ij} \times I_{t,ij}^m + Q_{l,t,j}^m + \sum_{k \in Dn_j^m} Q_{b,t,jk}^m \quad \forall t \in T, \forall j \in N^m \quad (21)$$

Where  $x$  and  $v$  refer to the reactance of the line and the square voltage magnitude,  $S_{1/2,j}^m$  is the set of SOPs connected to node  $j$  among the converter 1/2.  $P_p$ , and  $P_w$  refer to the generated power of PV and WT, respectively.  $P_{l,t,j}^m$ , and  $Q_{l,t,j}^m$  are the load demand of node  $j$ ,  $Dn_j^m$  is the set of its downstream nodes, and  $N^m$  is the set of total nodes in  $A_m$ .

The Dist Flow-based AC power flow is represented in (22) and (23) [28]. The permitted range of the square

voltage amplitude variation of the nodes is specified in (24).

$$v_{t,j}^m = v_{t,i}^m - 2(r_{ij} \times P_{b,t,ij}^m + x_{ij} \times Q_{b,t,ij}^m) + I_{t,ij}^m \times (r_{ij}^2 + x_{ij}^2) \quad \forall t \in T, \forall ij \in B^m \quad (22)$$

$$\left\| \begin{matrix} 2P_{b,t,ij}^m \\ 2Q_{b,t,ij}^m \\ I_{t,ij}^m - v_{t,i}^m \end{matrix} \right\| \leq I_{t,ij}^m + v_{t,i}^m \quad \forall t \in T, \forall ij \in B^m \quad (23)$$

$$v_{min} \leq v_{t,j}^m \leq v_{max} \quad \forall t \in T, \forall j \in N^m \quad (24)$$

Where the subscripts *min* and *max* show the minimum and maximum limits, respectively.

### 3. The proposed soft open point allocation method

In the proposed SOP allocation method, to show the willingness of MAADN areas to invest in each SOP plan, a new Fitness Index (FI) is defined in (25).

$$\eta_p^m = C_{to}^{m*} - C_{to,p}^m \quad (25)$$

Where subscript  $p$  refers to SOP plan  $p$ ,  $\eta_p^m$  is the FI of area  $m$  for plan  $p$ ,  $C_{to}^{m*}$  is the annual operating cost of area  $m$  without new SOPs, and  $C_{to,p}^m$  is the annual operating cost in the presence of new SOPs in plan  $p$ . Note that each plan represents both the site and size of new SOPs. As deduced from (25),  $\eta_p^m$  represents the annual net cost reduction of the area  $m$  in the plan  $p$ . Accordingly, if  $\eta_p^m$  is a negative number, the plan  $p$  is not cost-effective from the viewpoint of  $A_m$ . Therefore, only positive values  $\eta_p^m$  indicate the willingness of the area  $m$  to invest in plan  $p$ .

In the proposed method, when all the areas have announced their FIs for the plan  $p$ , the Net Fitness Index (NFI) of that plan is calculated using (26).

$$F_p = \sum_{m \in M} \eta_p^m - C_p^{SOP} \quad (26)$$

Where  $C_p^{SOP}$  is the annual investment cost of new SOPs in the plan  $p$ , and  $F_p$  is the NFI of the plan  $p$ , which expresses the Economic justification of the plan. The total annual SOP's investment cost of the plan  $p$  is defined in (27) [20].

$$C_p^{SOP} = c^{SOP} \frac{dr \times (1 + dr)^{lf}}{(1 + dr)^{lf} - 1} \sum_{s \in S_p} (S_{s,max}^p) \quad (27)$$

Where  $c^{SOP}$  is the per unit investment cost of the SOP, and  $lf$  is its lifetime.  $dr$  is the discount rate,  $S_{s,max}^p$  is the nominal apparent power of SOP  $s$  in plan  $p$ , and  $S_p$  is the set of all allocated SOPs in plan  $p$ .

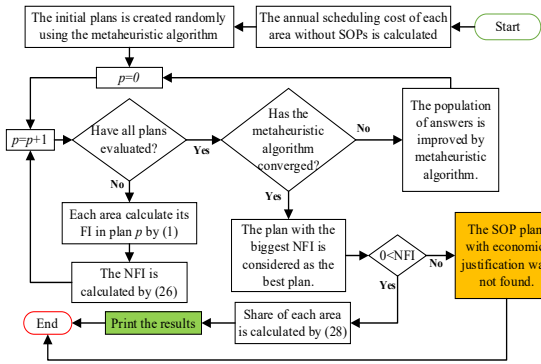


**Fig. 2.** Flowchart of the proposed decentralized SOP allocation method.

As it is obvious in (26), a plan  $p$  is economically justified only when  $F_p$  is positive. However, as the FPI becomes larger, the economic benefit of SOP outweighs its investment cost. Accordingly, in the proposed method, a metaheuristic-based method is developed to optimally allocate the SOP in the MAADN using the NFI. In this regard, both the site and size of SOPs are considered as the decision variables in each SOP plan. Then, their optimal values are simultaneously determined using a metaheuristic algorithm such as the GA or PSO to maximize the NFI.

After optimization, if the best obtained NFI ( $F_p$ ) is damaging the SOP allocation is not economically justified. Otherwise, the investment cost  $C_p^{SOP}$  should be fairly divided among MAADN areas. As mentioned, areas with a negative FI are not interested in investing in the installation of new SOPs. Therefore, the investment cost of SOPs should be covered only by the areas with positive FI, according to (28).

$$C_{SOP}^m = \begin{cases} C_p^{SOP} \frac{\eta_p^m}{\sum_{m \in M_p} \eta_p^m} & \eta_p^m > 0 \\ 0 & \eta_p^m \leq 0 \end{cases} \quad (98)$$

Where  $C_{SOP}^m$  is the annual SOP's investment cost of area  $m$ , and  $M_p$  is the set of areas with positive FI in plan  $p$ . As inferred from (28), in the proposed method, the investment costs are divided in proportion to their declared FI.

Fig. 2 represents the flowchart of the suggested SOP allocation strategy.

According to this figure, the main steps of the suggested strategy are summarized as follows:

As can be seen, the total daily operation cost of the MAADN is about 15665 \$. Areas 2 and 3, with 3957 \$ and 837 \$, respectively, have the highest and the lowest total net daily costs. Area 1 is the only area that is connected to the UN, and the cost of importing power from the UN to Area 1 is about 5510 \$. Area 5 has earned about 4456 \$ by selling power to Area 2. The highest CDG and power loss costs are in Area 5, with about 5657 \$ and 214 \$, which is due to exporting the generated powers of CDGs 8 and 9 to Area 2. Also, Area 2 should pay about 3306 \$ to Area 5 for importing power from it.

Step 1: Start.

Step 2: The annual scheduling cost of each area without SOPs ( $C_{to}^{m*}$ ) is calculated independently using (1).

Step 3: The initial SOP plans are created using a metaheuristic algorithm such as the GA or PSO.

Step 4: If all the SOP plans in the current iteration are evaluated, go to Step 8, otherwise go to Step 5.

Step 5: for plan  $p$ , the annual scheduling cost of each area considering the SOPs ( $C_{to,p}^m$ ) is calculated independently.

Step 6: Each area calculates its FI using (25).

Step 7: The NFI is calculated by (26).

Step 8: If the metaheuristic algorithm is converged, go to Step 9; otherwise, go to Step 4.

Step 9: If the best NFI is negative, go to Step 11, else to Step 10.

Step 10: The share of each area is determined according to (28), and go to Step 12.

Step 11: The SOP plan with economic justification was not found.

Step 12: End.

#### 4. Results and discussion

To evaluate the ability of the suggested decentralized planning method, it is applied to the modified IEEE 33-node and 123-node MAADNs. The data of these MAADNs is available in ref. [14]. The other SOP-planning data is summarized in Table 2.

**Table 2.** Used data of the SOP-planning

$c^{SOP}$ (\$/kVA)	$lf$ (year)	$dr$	$Zl_{1/2,s}^m$	$v_{min}$ (pu)	$v_{max}$ (pu)
308.8	7603.427335	0.08	0.02	0.95	1.05

All case studies are simulated in MATLAB on a laptop, 4 GB RAM, and Core i5-3210M 2.50 GHz CPU. The LSM of areas is modeled by YALMIP [29] and optimized by CPLEX 12.9.0.

IEEE 33-node

The diagram of the MAADN is depicted in Fig. 3. As shown; this MAADN consists of 5 autonomous areas  $A_1$  to  $A_5$ , which each of them is plotted by a certain color.

To investigate the impact of SOPs on the operating costs of an MAADN, this MAADN has been simulated in two scenarios: 1) without SOPs and 2) with SOPs.

In the first scenario, it is assumed that there is no SOP in the MAADN. Details of the daily operational cost of the MAADN for different areas are listed in Table 3. To compare the simulation results with ref. [14], the planning horizon is scaled to one day.

In this following, to evaluate the effect of the SOP on the operational cost, first, the SOP plan is assumed to be the same as the reference [14]. Then, the SOP allocation is optimized using the proposed decentralized method. It should be noted that to better compare the planning cost with the daily operation cost, the SOP investment costs have been scaled daily.

Fig. 4, shows two assumed installed SOPs in the MAADN. The site, size, and loss coefficients of the SOPs are the same as in [14]. The daily operation costs for all areas considering this SOP plans are listed in Table 4.



Table 3. The daily operation cost of the areas without SOPs.

Agent/Area (m)	$C_{to}^m$ (\$)	$C_{CDG}^m$ (\$)	$C_l^m$ (\$)	$C_{UN}^m$ (\$)	$C_A^m$ (\$)
1	7603.427335	0.000291402	105.0528379	5510.45203	1987.922176
2	3956.842489	555.7850854	94.47421979	0	3306.583184
3	836.8997714	3459.076686	64.23131806	0	-2686.408233
4	1852.083905	7.79042E-05	3.979283254	0	1848.104544
5	1415.696517	5657.968705	213.9294839	0	-4456.201672
MAADN	15664.95002	9672.830846	481.667143	5510.45203	0

Table 4. The daily operation cost of the areas in the SOP plan [14].

Agent/Area (m)	$C_{to}^m$ (\$)	$C_{CDG}^m$ (\$)	$C_l^m$ (\$)	$C_{UN}^m$ (\$)	$C_A^m$ (\$)
1	6211.788385	0.000844323	194.7075206	1593.845472	4423.234547
2	3907.033085	688.0135924	73.10606494	0	3145.913428
3	445.5073517	4736.760608	158.9683714	0	-4450.221628
4	2107.917878	0.000247888	75.98286561	0	2031.934765
5	1229.211055	6167.075193	212.996974	0	-5150.861112
MAADN	13901.45775	11591.85049	715.7617965	1593.845472	0

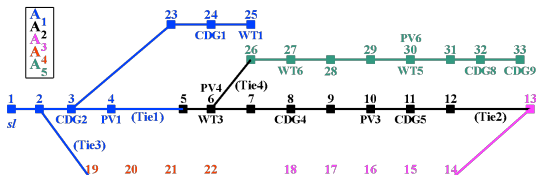


Fig. 3. The one-line diagram of modified IEEE 33-node ADN without SOP.

Table 5. The FI and share of each area in the SOP investment cost in the SOP plan proposed in [14].

Agent/Area (m)	$\eta_p^m$ (\$)	$C_{SOP}^m$ (\$)	Share (%)
1	1391.638951	118.7695094	68.91600403
2	49.80940423	4.250986579	2.466634827
3	391.3924198	33.40340944	19.38232726
4	-255.8339727	0	0
5	186.4854621	15.9156129	9.235033878
MAADN	1763.492264	172.3395183	100

Table 6. The best SOP plan of the proposed method.

SOP (s)	From	To	$S_{Smax,s}^m$ (kVA)
1	18	22	1400
2	25	29	1500

The comparative results of Tables 3 and 4 shows the installation of the SOPs according to the SOP plan of [14] has reduced the daily cost of the MAADN by 1763.492264 \$.

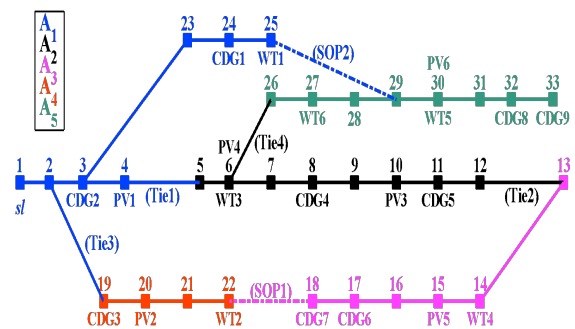


Fig. 4. The modified IEEE 33-node ADN with SOPs.

The FI of each area in this SOP plan is given in Table 5. The NFI ( $F_p$ ) of this plan is 1591.15 \$.

All the areas in the MAADN except area 4 have a positive FI. However, the daily operation cost of Area 4 has increased by 255.8339727 \$. Therefore, this area is not involved in providing SOP investment costs. The share of each area in the SOP investment cost is calculated according to (28) and given in the last column of Table 5. Area 1, with 68.916% and Area 2, with 2.4666%, respectively, have the biggest and smallest share in the SOP investment cost. In the presence of the SOPs, the operating costs of Areas 1 and 2 are respectively reduced by about 1391.64 and 49.80 \$. Sharing the SOP investment cost based on the proposed FI is one of the innovations of this paper. Using this index, the SOP investment cost is divided fairly between the MAADN areas.

In the following, to show the effect of the proposed NFI on the daily operating costs of areas, the site and size of two SOPs are determined by the suggested decentralized



Table 7. The daily operation cost, the FI, and the share of each area in the SOP investment cost.

Area (m)	$C_{Lo}^m$ (\$)	$C_{CDG}^m$ (\$)	$C_l^m$ (\$)	$C_{UN}^m$ (\$)	$C_A^m$ (\$)	$\eta_p^m$ (\$)	$C_{SOP}^m$ (\$)	Share (%)
1	5876.299	0.000	366.671	663.654	4845.974	1727.129	179.445	71.809
2	3901.081	704.963	69.593	0.000	3126.525	55.761	5.793	2.318
3	386.962	4967.735	140.380	0.000	-4721.152	449.937	46.747	18.707
4	2295.441	0.000	159.677	0.000	2135.765	-443.357	0.000	0.000
5	1243.349	6398.193	232.267	0.000	-5387.111	172.348	17.907	7.166
MAADN	13703.132	12070.891	968.587	663.654	0.000	1961.818	249.892	100.00

SOP allocation method. The best SOP plan with the highest NFI is given in Table 6 and is shown in Fig. 4.

As shown, the capacity of SOPs one and two are respectively increased to 1400 and 1500 kVA. The effect of these planes on the daily operation cost of the MAADN areas is summarized in Table 7.

A comparison between Tables 4 and 7 proves the superiority of the SOP allocation plan of the proposed method over the reference [14]. The NFI of the proposed plan is 1711.93 \$, which is 120.7773 \$ more than the SOP plan in [14].

IEEE 123-bus

The modified IEEE 123-node MAADN is depicted in Fig. 5. As shown; this MAADN consists of 5 areas that have been distinguished by a different color. All data of this MAADN is available in [14]. As described in Table 8, in this MAADN, it is assumed that 8 NOPs are candidates that can be replaced with the SOP.

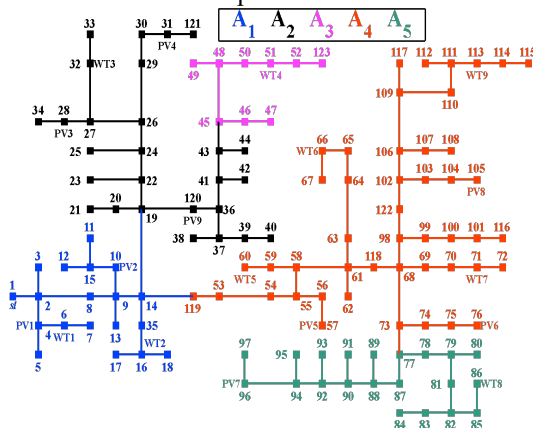


Fig. 5. The one-line diagram of IEEE 123-bus.

Table 8. The NOPs in the modified IEEE 123-bus.

NOP	From	To	NOP	From	To
1	55	95	5	47	66
2	117	123	6	18	97
3	40	67	7	38	119
4	49	121	8	57	91

Table 9. The planning result for the modified IEEE 123-node MAADN.

Algorithm	SOP (s)	From	To	$Ss_{max,s}^m$ (kVA)	$F_p$
GA	1	38	119	3800	3173.406
	2	18	97	1250	
PSO	1	38	119	3150	3163.158
	2	18	97	1700	

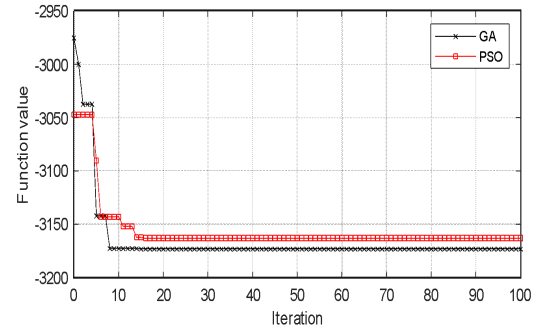


Fig. 6. The convergence curves of the PSO and GA.

The site and size of these SOPs should be determined with the consent of all MAADN areas in such a way that the required SOP allocation cost is covered by the agreement of these five agents. The proposed decentralized method can be implemented with all metaheuristic algorithms. To check the adaptability of metaheuristic algorithms with the proposed method and compare their performance, the SOP allocation of this MAADN is implemented with two GA and PSO algorithms.

The convergence curves for these two algorithms are depicted in Fig. 6. Note that the population size and maximum iteration of these algorithms are set to 10 and 100, respectively. Note, since the standard functions for PSO and GA in MATLAB are minimizing the objective function, the objective function is selected as  $-F_p$ .

As can be seen, in this MAADN, the GA has a better performance in comparison with the PSO. The SOP's planning results associated with these algorithms are summarized in Table 9.

As can be seen, the SOP locations in both algorithms are the same. However, the capacity of these two SOPs is varied. In the GA planning scheme, the areas agreed on the installation of 5050 kVA SOP, while in the PSO scheme, this agreement has been reduced to 4850 kVA. The NFI ( $F_p$ ) of the GA and PSO are respectively 3173.406 and 3163.158, which shows the superiority of the GA plan. The area costs in these two SOP plans are represented in Table 10.

Table 10. The comparison of planning results of the modified IEEE 123-node MAADN with two metaheuristic algorithms.

Area (m)	GA				PSO			
	$C_{to}^m$ (\$)	$C_{SOP}^m$ (\$)	$\eta_p^m$ (\$)	Share (%)	$C_{to}^m$ (\$)	$C_{SOP}^m$ (\$)	$\eta_p^m$ (\$)	Share (%)
1	-4662.57	423.32	3530.90	97.28	-4627.61	404.85	3495.94	96.87
2	-499.09	0.00	-3.96	0.00	-494.36	0.00	-8.69	0.00
3	355.14	0.12	0.99	0.03	355.14	0.11	0.99	0.03
4	-2885.11	11.72	97.78	2.69	-2899.28	12.96	111.95	3.10
5	-107.18	0.00	-17.15	0.00	-105.23	0.00	-19.11	0.00
MAADN	-7798.81	435.16	3608.56	100.00	-7771.33	417.92	3581.08	100.00

As can be seen, the total cost of the MAADN using the GA plan is reduced to -7798.81 \$, which is more than 27.48 \$ smaller than the PSO scheme. According to these results, Area 1 has the most IF ( $\eta_p^1$ ) and should pay 97.28% of the 435.16 \$ daily cost of the SOP installation. On the other hand, the FI of Areas 2 and 5 are negative, which means the share of these areas in the SOP planning scheme in both GA and PSO algorithms should be zero.

As can be inferred from this table, the proposed SOP planning method can effectively divide the SOP cost between the areas according to their FI.

## 5. Conclusion

In this research, a new decentralized SOP allocation method is presented for the first time. The proposed planning model can specify the optimal site and size of the SOPs in the MAADN and the share of each area in the SOP investment cost, simultaneously. Based on the results, in the MAADN, installing new SOPs may not be cost-effective from the viewpoint of some areas, such as agent 4 in the modified IEEE 33-node MAADN or areas 2 and 5 in the modified 123-node MAADN. In the suggested method, the SOP investment cost is divided among different areas based on the new proposed fitness index (FI) that represents the willingness of each area to the SOP plan. The net FI (NFI) index presented in this paper expresses the economic justification of the SOP plan well. The proposed method optimizes the SOP allocation by maximizing this novel index. According to the simulation results, the \$120.77 increase in the NFI has led to a reduction in the MAADN operating costs by more than \$198. By using the proposed method, the investment cost is fairly divided between areas, so that area one, which benefits more than other areas, should pay more than 97.28% of the SOP investment cost. In comparison, the share of area three is only 0.03%.

## References

- [1] Abdi, Hamdi. "A brief review of microgrid surveys, by focusing on energy management system." *Sustainability* vol. 15, 284 pp. 1-20, 2022. doi: <https://doi.org/10.3390/su15010284>.
- [2] Sharifian, Yeganeh, and Hamdi Abdi. "Multi-area economic dispatch problem: Methods, uncertainties, and future directions." *Renewable and Sustainable Energy Reviews* 191, 114093, 2024, doi: <https://doi.org/10.1016/j.rser.2023.114093>.
- [3] Abdul Kareem, H. Z., Hasan Mohammed, H., & Mohammed, A. A. (2024). Probabilistic analysis to solve the stability of a microgrid with uncertainty due to the presence of a wind turbine. *Australian Journal of Electrical and Electronics Engineering*, 21(2), 128-137. <https://doi.org/10.1080/1448837X.2024.2308981> <https://doi.org/10.1016/j.ijepes.2022.108788>.
- [4] Y. Shen, S. Zhang, M. Ding, H. Cheng, C. Li, and D. Liu, "Expansion Planning of Soft Open Points Based Distribution System Considering EV Traffic Flow," *IEEE Transactions on Industry Applications*, vol. 60, no. 1, pp. 1229-1239, 2024, doi: 10.1109/TIA.2023.3293496.
- [5] H. Ji, C. Wang, P. Li, F. Ding, and J. Wu, "Robust Operation of Soft Open Points in Active Distribution Networks With High Penetration of Photovoltaic Integration," *IEEE Transactions on Sustainable Energy*, vol. 10, no. 1, pp. 280-289, 2019, doi: <https://doi.org/10.1109/TSTE.2018.2833545>.
- [6] X. Jiang, Y. Zhou, W. Ming, P. Yang, and J. Wu, "An Overview of Soft Open Points in Electricity Distribution Networks," *IEEE Transactions on Smart Grid*, vol. 13, no. 3, pp. 1899-1910, 2022, doi: 10.1109/TSG.2022.3148599.
- [7] Y. Qi, Y. Li, W. Li, H. Deng, and Y. Tang, "Autonomous Control of Soft Open Point for Distribution Network Reliability Enhancement," *IEEE Journal of Emerging and Selected Topics in Power Electronics*, pp. 1-1, 2023, doi: 10.1109/JESTPE.2023.3253480.
- [8] C. Han, S. Cho, S.-G. Song, and R. R. Rao, "Regression model-based adaptive receding horizon control of soft open points for loss minimization in distribution networks," *International Journal of Electrical Power & Energy Systems*, vol. 151, p. 109130, 2023, doi: <https://doi.org/10.1016/j.ijepes.2023.109130>.
- [9] C. Lou, J. Yang, E. Vega-Fuentes, N. K. Meena, and L. Min, "Multi-terminal phase-changing soft open point SDP modeling for imbalance mitigation in active distribution networks," *International Journal of Electrical Power & Energy Systems*, vol. 142, p. 108228, 2022, doi: <https://doi.org/10.1016/j.ijepes.2022.108228>.
- [10] S. Rezaeian-Marjani, V. Talavat, and S. Galvani, "Impact of soft open point (SOP) on distribution network predictability," *International Journal of Electrical Power & Energy Systems*, vol. 136, p. 107676, 2022, doi: <https://doi.org/10.1016/j.ijepes.2021.107676>.
- [11] C. Lv, R. Liang, G. Zhang, X. Zhang, and W. Jin, "Energy accommodation-oriented interaction of active distribution network and central energy station considering soft open points," *Energy*, vol. 268, p. 126574, 2023, doi: <https://doi.org/10.1016/j.energy.2022.126574>.
- [12] W. Huang, C. Gao, R. Li, R. Bhakar, N. Tai, and M. Yu, "A Model Predictive Control-Based Voltage Optimization Method for Highway Transportation Power Supply Networks With Soft Open Points," *IEEE Transactions on Industry Applications*, vol. 60, no. 1, pp. 1141-1150, 2024, doi: 10.1109/TIA.2023.3296574.
- [13] T. Qian, W. Ming, C. Shao, Q. Hu, X. Wang, J. Wu, and Z. Wu, "An Edge Intelligence-Based Framework for Online Scheduling of Soft Open Points With Energy Storage," *IEEE Transactions on Smart Grid*, vol. 15, no. 3, pp. 2934-2945,

- 2024, doi: 10.1109/TSG.2023.3330990.
- [14] H. Bastami, M. R. Shakarami, and M. Doostizadeh, "A decentralized cooperative framework for multi-area active distribution network in presence of inter-area soft open points," *Applied Energy*, vol. 300, p. 117416, 2021, doi: <https://doi.org/10.1016/j.apenergy.2021.117416>.
- [15] H. Ji, C. Wang, P. Li, G. Song, and J. Wu, "SOP-based islanding partition method of active distribution networks considering the characteristics of DG, energy storage system and load," *Energy*, vol. 155, pp. 312-325, 2018, doi: <https://doi.org/10.1016/j.energy.2018.04.168>.
- [16] P. Li, J. Ji, H. Ji, G. Song, C. Wang, and J. Wu, "Self-healing oriented supply restoration method based on the coordination of multiple SOPs in active distribution networks," *Energy*, vol. 195, p. 116968, 2020, doi: <https://doi.org/10.1016/j.energy.2020.116968>.
- [17] X. Yang, Z. Zhou, Y. Zhang, J. Liu, J. Wen, Q. Wu, and S. Cheng, "Resilience-Oriented Co-Deployment of Remote-Controlled Switches and Soft Open Points in Distribution Networks," *IEEE Transactions on Power Systems*, vol. 38, no. 2, pp. 1350-1365, 2023, doi: 10.1109/TPWRS.2022.3176024.
- [18] J. Zhang, A. Foley, and S. Wang, "Optimal planning of a soft open point in a distribution network subject to typhoons," *International Journal of Electrical Power & Energy Systems*, vol. 129, p. 106839, 2021, doi: <https://doi.org/10.1016/j.ijepes.2021.106839>.
- [19] C. Wang, G. Song, P. Li, H. Ji, J. Zhao, and J. Wu, "Optimal siting and sizing of soft open points in active electrical distribution networks," *Applied Energy*, vol. 189, pp. 301-309, 2017, doi: <https://doi.org/10.1016/j.apenergy.2016.12.075>.
- [20] J. Wang, N. Zhou, C. Y. Chung, and Q. Wang, "Coordinated Planning of Converter-Based DG Units and Soft Open Points Incorporating Active Management in Unbalanced Distribution Networks," *IEEE Transactions on Sustainable Energy*, vol. 11, no. 3, pp. 2015-2027, 2020, doi: 10.1109/TSTE.2019.2950168.
- [21] M. Ehsanbakhsh and M. S. Sepasian, "Simultaneous siting and sizing of Soft Open Points and the allocation of tie switches in active distribution network considering network reconfiguration," *IET Generation, Transmission & Distribution*, vol. 17, no. 1, pp. 263-280, 2023, doi: <https://doi.org/10.1049/gtd2.12683>.
- [22] M. A. Saaklayen, X. Liang, S. O. Faried, L. Martirano, and P. E. Sutherland, "Soft Open Point-Based Service Restoration Coordinated With Distributed Generation in Distribution Networks," *IEEE Transactions on Industry Applications*, vol. 60, no. 2, pp. 2554-2566, 2024, doi: 10.1109/TIA.2023.3332584.
- [23] M. Deakin, I. Sarantakos, D. Greenwood, J. Bialek, P. C. Taylor, and S. Walker, "Comparative analysis of services from soft open points using cost-benefit analysis," *Applied Energy*, vol. 333, p. 120618, 2023, doi: <https://doi.org/10.1016/j.apenergy.2022.120618>.
- [24] Z. Huang, Y. Zhang, and S. Xie, "A comprehensive strategy for the distribution network resilience enhancement considering the time-varying behaviors of typhoon path," *Electric Power Systems Research*, vol. 214, p. 108819, 2023, doi: <https://doi.org/10.1016/j.eprsr.2022.108819>.
- [25] J. Li, S. Ge, S. Zhang, Z. Xu, L. Wang, C. Wang, and H. Liu, "A multi-objective stochastic-information gap decision model for soft open points planning considering power fluctuation and growth uncertainty," *Applied Energy*, vol. 317, p. 119141, 2022, doi: <https://doi.org/10.1016/j.apenergy.2022.119141>.
- [26] P. Khalouie, P. Alemi, and M. Beiraghi, "An Optimal Scenario-Based Scheduling Method for an SOP-included Active Distribution Network Considering Uncertainty of Load and Renewable Generations," *Scientia Iranica*, pp. -, 2023, doi: 10.24200/sci.2023.60823.7005.
- [27] H. Bastami, M. R. Shakarami, and M. Doostizadeh, "Optimal scheduling of a reconfigurable active distribution network with multiple autonomous microgrids," *Electric Power Systems Research*, vol. 201, p. 107499, 2021, doi: <https://doi.org/10.1016/j.eprsr.2021.107499>.
- [28] M. Farivar and S. H. Low, "Branch Flow Model: Relaxations and Convexification—Part I," *IEEE Transactions on Power Systems*, vol. 28, no. 3, pp. 2554-2564, 2013, doi: <https://doi.org/10.1109/TPWRS.2013.2255317>.
- [29] J. Lofberg, "YALMIP : a toolbox for modeling and optimization in MATLAB," in *2004 IEEE International Conference on Robotics and Automation (IEEE Cat. No.04CH37508)*, 2-4 Sept. 2004 2004, pp. 284-289, doi: <https://doi.org/10.1109/CACSD.2004.1393890>.